



Cite this: *Mater. Adv.*, 2024, 5, 2655

## Anti-corrosion applications of 2D transition metal based layered materials

Yuqin Tian,<sup>a</sup> Qiaoxin Yang,<sup>a</sup> Wei Li,<sup>a</sup> Yuan Gong,<sup>ID</sup><sup>a</sup> Qiuping Zhao,<sup>a</sup> Chunlei Li<sup>\*a</sup> and Xinxin Sheng<sup>ID</sup><sup>\*bc</sup>

Metal corrosion causes great economic losses, wastes resources, pollutes the environment and damages personal safety. With the birth of the two-dimensional (2D) material graphene, there has been an upsurge in research on two-dimensional materials. Because of their excellent physical and chemical properties, two-dimensional materials have great application potential and prospects in the field of metal corrosion protection. Two-dimensional transition metal layered materials including layered double hydroxides (LDHs), transition metal carbonitrides (MXenes) and transition metal dichalcogenides (TMDs) have also received extensive attention. This article briefly introduces the above three two-dimensional transition metal layered materials. The current application status of LDHs, TMDs and MXenes in the field of metal anti-corrosion is focused on. Some studies that can be carried out in the future with the two-dimensional transition metal layered materials in corrosion prevention are proposed.

Received 28th October 2023,  
Accepted 6th February 2024

DOI: 10.1039/d3ma00919j

rsc.li/materials-advances

## 1. Introduction

In 2004, Andre K. Geim and Konstantin Novoselov obtained graphene by a simple exfoliation method.<sup>1</sup> Two-dimensional nanomaterials have attracted extensive research attention since then.<sup>2,3</sup> Among them, two-dimensional transition metal layered materials including layered double hydroxides (LDHs),<sup>4–7</sup> transition metal dichalcogenides (TMDs)<sup>8–11</sup> and transition metal carbonitrides (MXenes)<sup>12–16</sup> have also received extensive attention. Two-dimensional transition metal layered materials have a large specific surface area,<sup>17</sup> excellent physical and chemical properties,<sup>18–21</sup> and have been widely used in a lot of fields, including energy storage and conversion,<sup>22–25</sup> catalysis,<sup>26–29</sup> biomedicine,<sup>30,31</sup> metal corrosion and prevention,<sup>32,33</sup> flame retardants,<sup>34–36</sup> etc. This article focuses on two-dimensional transition metal layered materials and their applications in corrosion prevention.

### 1.1. Layered double hydroxides (LDHs)

LDHs, commonly known as hydrotalcites, are typical two-dimensional layered materials composed of two or more metal

elements.<sup>37,38</sup> In 1942, Feitkhnacht *et al.* first prepared LDHs through the co-precipitation method by reacting magnesium chloride, aluminum chloride, *etc.* with hydroxide. With extensive research, the structure of LDHs has been clarified. The synthesis method has been continuously proposed, and the application field of LDHs is also broadened. LDHs consist of a positively charged brucite-like layer and an interlayered region containing negatively charged anions or solvation molecules.<sup>39</sup> The general structural formula of LDHs is  $[M_{1-x}^{2+}M_x^{3+}(OH)_2]^{x+} \cdot (A^{n-})_{x/n} \cdot yH_2O$ , where  $M^{2+}$  and  $M^{3+}$  represent divalent and trivalent metal cations in the laminate,  $A^{n-}$  refers to the interlayer anion, and  $y$  is the amount of crystal water.<sup>40–44</sup> The structure of LDHs is shown in Fig. 1.<sup>45</sup>

The anions between the layers can maintain the charge balance, making LDHs, as a whole, electrically neutral. LDHs are characteristic of the exchange of interlayer anions with external counterparts, which is ascribed to the weak or trivial crosslinking between the host layers.<sup>46</sup> The host laminates of LDHs are orderly combined with interlayer anions through electrostatic interactions, van der Waals forces, and hydrogen bonds. The types of metal elements in the laminates and the interlayer anions can be adjusted to realize the controllable synthesis of LDHs. In addition, the interlayer anions of LDHs are exchangeable, which allows the synthesis of a variety of functional anion-intercalated LDHs. LDHs also have thermal stability and structural memory effects. LDHs have been widely used in biomedicine, catalysis, sensors, optoelectronic devices, thin films, corrosion resistance and other fields.<sup>47–49</sup>

The preparation methods of LDHs include the co-precipitation method, the roasting reduction method, the ion

<sup>a</sup>College of Petrochemical Technology, Lanzhou University of Technology, Lanzhou 730050, P. R. China. E-mail: licl@lut.edu.cn, 20220045@lut.edu.cn, 232081700023@lut.edu.cn, 222085602026@lut.edu.cn, yuangong@lut.edu.cn, 1134743502@qq.com

<sup>b</sup>Department of Polymeric Materials and Engineering, School of Materials and Energy, Guangdong University of Technology, Guangzhou, 510006, P. R. China. E-mail: xinxin.sheng@gdut.edu.cn, cexxsheng@gmail.com

<sup>c</sup>Guangdong Provincial Key Laboratory of Functional Soft Condensed Matter, Guangdong University of Technology, Guangzhou 510006, P. R. China



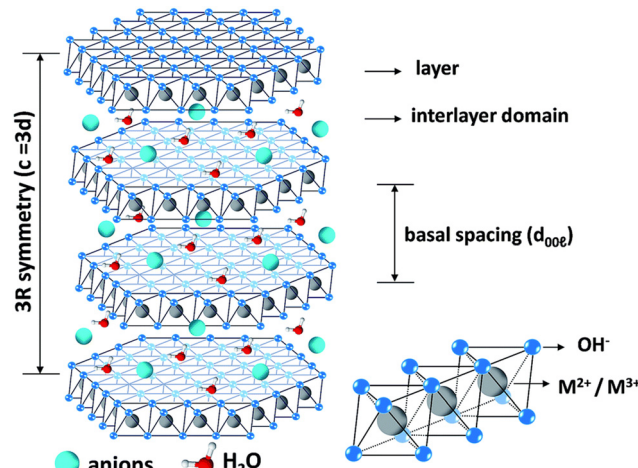


Fig. 1 The structure of LDHs. Reproduced with permission from ref. 45. Copyright 2021 Royal Society of Chemistry.

exchange method, the hydrothermal method and the sol-gel method and so on. The co-precipitation method is to mix the metal salt solution constituting the laminate with the alkali solution under certain conditions to nucleate, and then crystallize at a certain temperature to form LDHs, which is the most commonly used method for preparing LDHs.<sup>50–52</sup> However, the preparation of LDHs by the co-precipitation method has problems such as poor crystal form and uneven particle size. The hydrothermal method uses insoluble oxides and hydroxides of metal ions and alkaline solutions as raw materials to prepare LDHs under high temperature and pressure conditions.<sup>53</sup> Compared with the co-precipitation method, LDHs prepared by the hydrothermal method have better crystal form and a uniform particle size distribution. Based on the exchangeability of LDH interlayer anions, the ion exchange method replaces anions and inserts the required anions, thereby endowing LDHs with new properties.<sup>54,55</sup> Based on the structural memory of LDHs, the metal oxide after LDH roasting is placed in an aqueous solution of the anion to be intercalated at a certain temperature to rebuild the layered structure of LDHs. This method can prepare LDHs with different anions but the same structure as the initial structure.<sup>56,57</sup>

## 1.2. Transition metal carbonitrides (MXenes)

In 2011, Yury Gogotsi *et al.* reported a two-dimensional material obtained by removing Al in  $\text{Ti}_3\text{AlC}_2$  with hydrofluoric acid and named it MXene.<sup>58</sup> The precursor of MXenes is a class of ternary layered compounds (MAX) with a unified chemical formula  $\text{M}_{n+1}\text{AX}_n$ , where M is a transition metal, A is III or IV groups elements, X is C or N atoms, and  $n = 1, 2, 3, \text{etc.}$ <sup>59,60</sup> In MAX, M atomic layers and A atomic layers are alternately arranged to form a close-packed hexagonal layered structure, and X fills the octahedral gaps (as shown in Fig. 2).<sup>61</sup>

In MAX, there is a strong covalent bond or ionic bond between M-X, and a weak metal bond between M-A. So MXene materials can be obtained by etching the atomic layer of A.<sup>62</sup> MXenes have hydrophilicity,<sup>63</sup> great biocompatibility and

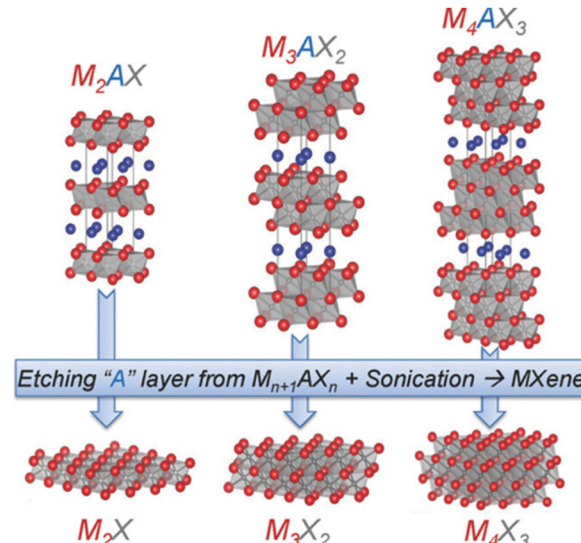


Fig. 2 Structures of MAX and the corresponding structures of MXenes. Reproduced with permission from ref. 61. Copyright 2014 Wiley.

electrochemical performance, and high conductivity.<sup>64,65</sup> Due to the unique physical and chemical properties of MXenes, they have received extensive attention and research studies in the fields of sensors, biomedicine, catalysis, energy storage and conversion, and multifunctional polymer composites.<sup>66–71</sup> The current methods for preparing MXenes mainly include etching and bottom-up methods. HF is the first reported etchant for the successful preparation of MXenes.<sup>72</sup> However, due to the strong corrosiveness and high toxicity of HF, with the deepening of MXene research, the process of preparing MXenes has gradually developed in a greener and more environmentally friendly direction. The currently reported etchants include solutions of LiF and HCl, molten fluoride salts, molten transition metal halides, high-temperature alkali solutions, *etc.*<sup>73–75</sup> In addition, electrochemical etching can also be used to prepare MXenes, which provides a new idea for the preparation of MXenes.<sup>76</sup> The bottom-up approach is to prepare MXenes by chemical vapor deposition, which can obtain MXenes with large areas, high quality and fewer defects.

## 1.3. Transition metal dichalcogenides (TMDs)

TMDs have a graphene-like two-dimensional layered structure, and the general formula can be written as  $\text{MX}_2$ , where M represents a transition metal element (such as Mo, W, Ti, *etc.*), and X refers to chalcogen elements (S, Se and Te).<sup>77,78</sup> The structure of a single-layer TMD generally presents an X-M-X sandwich structure. The TMD layers are connected by weak van der Waals forces, and there are strong chemical bonds in each layer plane. In 1963, Robert Frindt obtained an ultrathin  $\text{MoS}_2$  layer by cutting from the surface of a large  $\text{MoS}_2$  crystal.<sup>79</sup> TMDs have now been widely used in optoelectronic devices, catalysis, quantum information, energy storage, corrosion resistance and other fields.<sup>80–83</sup>

The top-down preparation methods of 2D TMDs mainly include mechanical exfoliation, liquid-phase ultrasonic exfoliation,



and intercalation-based exfoliation.<sup>84</sup> The method of mechanical exfoliation is easy to operate, but the size and number of layers prepared are uncontrollable. In addition, this method cannot prepare TMDs on a large scale. Liquid exfoliation refers to the direct peeling of TMDs by destroying the van der Waals interaction between TMD layers using ultrasonic waves in a solvent. Intercalation-based exfoliation is used to prepare TMDs by intercalating ions or molecules to increase the interlayer distance and weaken the interlayer interaction. Bottom-up preparation methods include the hydrothermal method and the chemical vapor deposition (CVD) method.

## 2. Corrosion

### 2.1. Corrosion mechanism and corrosion damage

Metal materials can easily interact with the surrounding environment to cause metal corrosion, resulting in the loss and degradation of metal materials.<sup>85</sup> The huge harm caused by metal corrosion involves various aspects such as public health safety, human health, economic loss, waste of resources, *etc.* Metals are purified from metal ores by the metal smelting technology.<sup>86</sup> From a thermodynamic point of view, the ore exists in a thermodynamically stable state. In the process of extracting pure metal, energy is forced into the ore, so the metal is in a thermodynamically unstable state. Metal corrosion is a process that releases energy and causes the metal to return to the lowest energy stable state. During this process, metal materials would lose their properties. The most common type of corrosion is electrochemical corrosion. The metal comes into contact with the electrolyte solution to form a corroded primary battery, resulting in the destruction of the metal materials and the inability to do any useful work for the outside world.<sup>87</sup> Electrochemical corrosion includes three processes, the anodic process, cathodic process, and current loop. Among them, the anode process is that a metal substrate dissolves when it comes into contact with the corrosive medium ( $M \rightarrow M^{n+} + ne^-$ ), and then enters the media in the form of metal ions. The cathode process is that the electrons flowing from the anode are absorbed by oxygen and hydrogen ions, *etc.* ( $O_2 + 2H_2O + 4e^- \rightarrow 4OH^-$ ;  $2H^+ + 2e^- \rightarrow H_2 \uparrow$ ). There is a current flowing in the middle, forming a current loop.<sup>88</sup> As long as any one of these three processes is stopped, corrosion would be prevented. Therefore, metal corrosion prevention measures are aimed at blocking these three processes.

### 2.2. Corrosion prevention measures

Metal corrosion prevention measures include changing the inherent structure of the metal,<sup>89</sup> improving the corrosion environment,<sup>90</sup> electrochemical protection including cathodic protection and anodic protection,<sup>91,92</sup> and metal surface coatings. Forming a covering layer on the metal surface, including metal plating, chemical conversion coatings, polymer coatings, *etc.*, can isolate the contact between the metal materials and corrosive media to greatly prevent the damage of corrosive media.<sup>93-95</sup>

The incorporation of 2D nanomaterials in metal corrosion prevention has been extensively studied. Due to the layered structure, large specific surface area, excellent impermeability, and mechanical properties of two-dimensional materials, they can play a labyrinth effect in coatings. This article mainly focuses on the application of 2D transition metal layered materials in metal corrosion prevention.<sup>96</sup>

## 3. Applications of 2D transition metal layered materials in corrosion prevention

### 3.1. Applications of LDHs in corrosion prevention

Due to the adjustable types of metal ions and anions in LDHs, LDHs can be controllably prepared. In addition, LDHs have excellent ion exchange capacity due to their special 2D structure, which also provides the possibility to insert corrosion inhibitors in the LDH layers.<sup>97,98</sup> LDHs can be doped into polymer coatings to improve the performance of polymer coatings, and can also be directly applied to the surface of metal substrates in the form of conversion coatings to protect metals.

**3.1.1. LDH conversion coatings.** Chemical conversion coating is an important pretreatment step for metal substrates before industrial application. Conversion coatings can be used as intermediate layers between polymer coatings and metal substrates, and can also directly protect metal substrates from corrosion damage. Chemical conversion coatings have been widely used in aerospace, building materials, automotive appliances, and other fields. The most important method for forming LDH conversion coatings is the *in situ* growth method, which can directly form vertically oriented LDH coatings on metal surfaces.<sup>99</sup> The *in situ* growth method can form a strong chemical bond between the conversion coating and the surface of the metal substrate, which makes the conversion coatings have strong adhesion.<sup>100</sup> The application research of LDH conversion coatings on the surface of magnesium alloy and aluminum alloy substrates is more extensive.

Bouali *et al.* proposed the mechanism of ZnAl layered double hydroxide conversion coating on the surface of the AA2024-T3 aluminum alloy.<sup>101</sup> Their research work proposed that the LDH conversion coating was controlled by diffusion reactions, which are divided into three stages. In the first stage, the original oxide layer rapidly transformed into the AlOOH intermediate layer. As the pH increased, the AlOOH intermediate layer was partially dissolved, and  $Al(OH)^{4-}$  reacted with  $Zn(OH)^{2+}$  to form LDH flakes. The LDH flakes generated continued to grow to form LDH conversion coatings in the third stage and protect the surface of the aluminum alloy substrate from corrosion. Zhao *et al.* prepared LDH coatings containing Ce ions on the surface of the AZ31 magnesium alloy. In addition, their team also successfully prepared 8-hydroxy-quinoline (8HQ) intercalated Mg-Al LDH coatings on the surface of the AZ31 magnesium alloy.<sup>102</sup> The anti-corrosion mechanism of the LDH conversion coating in the magnesium alloy is shown in Fig. 3. LDHs have anion exchange capacity;



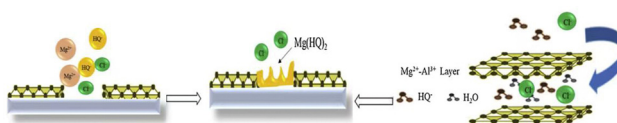


Fig. 3 Mechanism of corrosion inhibition of the 8HQ intercalated Mg-Al LDH coating on AZ31. Reproduced with permission from ref. 102. Copyright 2020 Elsevier.

$\text{Cl}^-$  in the corrosive media can be exchanged with 8HQ, which would greatly reduce the damage of the corrosive media to the metal substrate. Secondly, 8HQ can also chelate with  $\text{Mg}^{2+}$  to form insoluble precipitate  $\text{Mg}(\text{HQ})_2$ , which can seal the defects of LDH conversion coatings to further reduce the occurrence of corrosion reactions. The effective synergistic effect of corrosion inhibitors and LDHs provides a new idea for the corrosion resistance of magnesium alloys.

Due to the defects of the simply prepared LDH conversion coatings and the poor performance of the coatings, they cannot provide more long-term stable protection for the metal substrates. Therefore, research studies on LDH conversion coatings have expanded to multifunctional composite coatings, such as endowing the coatings with self-healing, self-cleaning, and superhydrophobic functions to provide longer-term stable and effective protection for the LDH coatings.<sup>103,104</sup> Cao *et al.* prepared a layered ZnAl-LDH-La LDH coating with superhydrophobic function on the surface of an aluminum substrate.<sup>105</sup> The ZnAl-LDH coating was first prepared by a hydrothermal method and then soaked in sodium laurate solution to endow the coating with superhydrophobic properties. The prepared coating has long-term stable corrosion resistance performance. Zhang *et al.* prepared aspartic acid-intercalated Li-Al LDH conversion coatings on 6N01 aluminum alloy. The conversion coatings are dense and uniform, and have self-healing properties.<sup>106</sup> Mohammadi *et al.* used a one-step hydrothermal method to prepare a Zn-Al LDH conversion coating intercalated with benzimidazole on the surface of the AA2024-T3 metal substrate.<sup>107</sup> The modification of the corrosion inhibitor benzimidazole molecule effectively improved the corrosion resistance of LDH conversion coatings. Wang *et al.* used the hydrothermal method to grow LDH coatings *in situ* by plasma electrolytic oxidation (PEO) (PEO-LDHs) and then modified the PEO-LDH composite coating with sodium dodecyl sulfate (SDS) using an anion exchange reaction (PEO-LDHs-SDS). The corrosion resistance mechanism of the PEO-LDHs-SDS composite coating is shown in Fig. 4. Firstly, LDHs can fill the defects in the PEO coating and capture  $\text{Cl}^-$  through anion exchange. Secondly, SDS can endow the coatings with superhydrophobic properties.<sup>108</sup>

Jian *et al.* *in situ* generated sodium pyrithione modified LDH coatings on the surface of an aluminum alloy, which can improve the corrosion resistance and antifouling performance of aluminum alloy 7075 at the same time.<sup>109</sup> Li *et al.* deposited NiP coating on the surface of Mg-Li alloy, then grew MgAl LDHs *in situ* on an NiP coating, and finally modified the NiP/MgAl LDH double-layer coating with stearic acid (@SA)

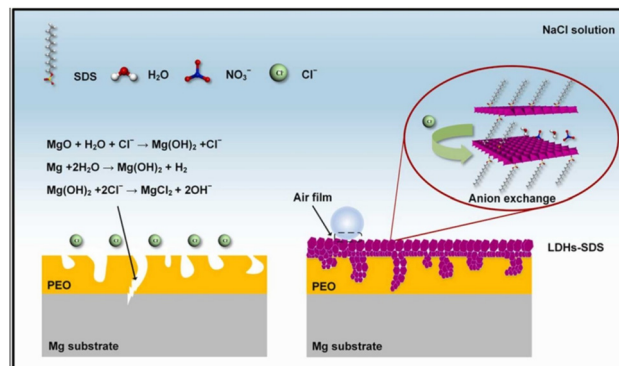


Fig. 4 The corrosion resistance mechanism of the PEO-LDHs-SDS composite coating. Reproduced with permission from ref. 108. Copyright 2022 Elsevier.

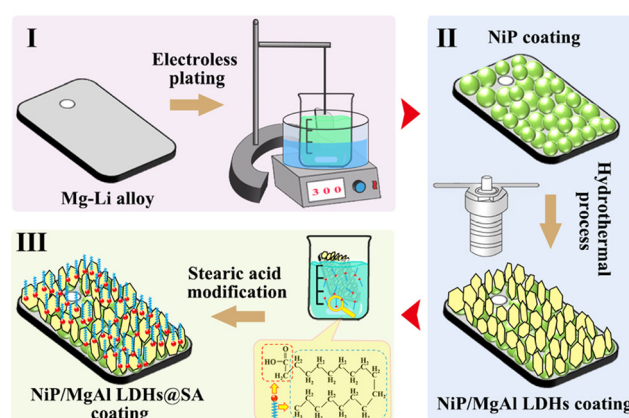


Fig. 5 The preparation process of the NiP/MgAl LDHs@SA coating. Reproduced with permission from ref. 110. Copyright 2023 Elsevier.

to achieve the superhydrophobic function of the composite coatings.<sup>110</sup> The preparation process of the NiP/MgAl LDHs@SA coating is shown in Fig. 5. On the one hand, the LDHs generated *in situ* can fill the defects of NiP coating, and on the other hand, LDHs can capture the corrosion ions. Furthermore, superhydrophobic modification would further inhibit the occurrence of corrosion. The construction of the double coatings provides new ideas for metal corrosion prevention methods. The above works confirm that multifunctional composite coatings can protect metal substrates from damage for a longer period of time.

In addition, ionic liquids, octadecyl-trimethoxy-silane, salicylic acid, *etc.* have all been reported for the modification of LDHs to enhance the corrosion resistance of LDH coatings.<sup>111-113</sup> Other two-dimensional materials such as graphene oxide, transition metal carbonitrides and metal-organic frameworks can also form composite coatings with LDHs to achieve the purpose of synergistically protecting metal substrates from corrosion.<sup>114-116</sup> LDH coatings will be more widely used in future.

**3.1.2. Applications of LDHs in polymer coatings.** A polymer is a material with a high molecular compound as the main component, which is applied to the metal surface to prevent the



metal substrates from being damaged by corrosion.<sup>117–119</sup> Multiple protection mechanisms of polymer coatings on metal substrates are realized through flexible design and formulation. The solvents of the traditional polymer coatings used are organic solvents that contain volatile organic compounds, which are very harmful to the environment and human health. As environmental protection policies become more and more stringent, organic coatings are developing in the direction of water-based coatings. Water-based coatings are environmentally friendly and safer, and the cost of raw materials is also reduced. Polymer coatings have certain defects, especially water-based polymer coatings have more defects due to the volatilization of water and the incompatibility of coating-forming substances.<sup>120</sup> In addition, due to the wide range of coatings used, polymer coatings inevitably suffer from various types of corrosion damage during service, when exposed to various environments. It causes physical, chemical and mechanical damage to the coatings. The barrier protection mechanism of the coatings depends on the ion impermeability, so the research on the improvement of corrosion resistance is of far-reaching significance.

LDHs can act as fillers in polymer coatings due to their 2D lamellar structure and anion exchange capacity. On the one hand, LDHs can fill the defects of polymer coatings and block the penetration of corrosive media. On the other hand, they have the ability to capture  $\text{Cl}^-$  to slow down the occurrence of corrosion reactions. Zhang *et al.* designed and constructed a trifunctional filler to improve the corrosion resistance of epoxy coatings (EP). Basalt scales (Bt) were firstly modified with polydopamine (PDA) (Bt@PDA), and then molybdate intercalated LDH (LM) was grown *in situ* on the surface of Bt@PDA (Bt@PDA@LM).<sup>121</sup> The protection mechanism for Bt@PDA@LM/EP coating is shown in Fig. 6. In addition to the blocking effect on corrosive media and the trapping effect on  $\text{Cl}^-$ , the molybdate corrosion inhibitor released by LDH due to anion exchange further inhibited the occurrence of corrosion.

The work of Wang *et al.* reported that sodium tripolyphosphate intercalated LDHs as fillers also effectively improved the corrosion resistance of the waterborne epoxy coating.<sup>122</sup>

The tripolyphosphate ions released by anion exchange have the effect of chelating iron ions to passivate the metal surface, thereby preventing the metal substrate from being damaged by corrosive media. Xu *et al.* prepared zeolitic imidazolate framework-8 (ZIF-8) *in situ* on the surface of Zn-Al LDHs and then loaded the corrosion inhibitor 1H-benzotriazole (BTA) PVB/(LDH/ZIF-8@BTA).<sup>123</sup> LDH/ZIF-8@BTA were filled in the polyvinyl butyral (PVB) coatings to effectively enhance the passive and active anti-corrosion performance of the composite coatings for metal substrates. LDH-conductive polymer composites can also achieve synergistic anti-corrosion effects. Chetan B. Pawar *et al.* applied amino silane to surface treat Zn-Al LDHs and Mg-Al LDHs synthesized by the precipitation method, and then grafted conductive polymers polyaniline (PANI), poly-orthoanisidine (POA), and PANI-POA copolymer onto the surface of LDHs.<sup>124</sup> The addition of the synthesized LDH-conductive polymer composites to epoxy-polyamide based coatings can enhance the pencil hardness, scratch resistance, and corrosion resistance of coatings. LDHs after functional modification can better play a corrosion-resistant role in polymer coatings. Therefore, LDHs have great application prospects in conversion coatings or as nanofillers for polymer coatings.<sup>125</sup>

### 3.2. Applications of MXenes in corrosion prevention

There have been a lot of research works reporting the application of MXenes in corrosion prevention. Due to the large specific surface area, excellent mechanical properties and many other superior properties, MXenes can exert the labyrinth effect in polymer coatings to block the penetration of corrosive media. However, there are also some problems in applying MXenes directly into polymer coatings.<sup>126</sup> MXenes are prone to agglomerate in polymer coatings, resulting in poor dispersion.<sup>127</sup> MXenes are also easily oxidized and have poor stability.<sup>128</sup> Moreover, the direct addition of MXenes may cause galvanic corrosion due to the conductivity of MXenes.<sup>129</sup> Therefore, before MXenes are added to the polymer coatings, they need to be modified to achieve great dispersion to better protect the metal substrates. MXenes can be modified through covalent or non-covalent interactions.

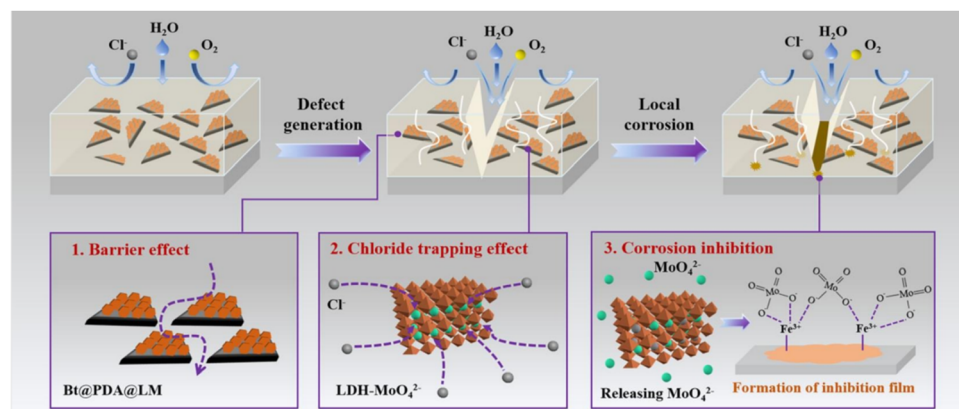


Fig. 6 The protection mechanism of the Bt@PDA@LM/EP coating. Reproduced with permission from ref. 121. Copyright 2022 Elsevier.



The construction of self-healing coatings enables the coatings to actively protect against corrosion when damaged. Sun *et al.* combined mesoporous silica nanoparticles loaded tannic acid corrosion inhibitor onto the MXene surface as nanofillers for epoxy coatings.<sup>130</sup> In addition to the passive shielding effect on corrosive media, when the coatings were damaged, the corrosion inhibitor tannic acid would be released and react with iron ions to form a self-healing film to achieve active protection of the metal substrate.<sup>131</sup> The strategy adopted by Yan *et al.* was to encapsulate benzotriazole as the corrosion inhibitor and self-healing agent in a 2-methylimidazole zinc salt (ZIF-8) nanocontainer (ZB), and then load the ZB on the amino-functionalized  $\text{Ti}_3\text{C}_2\text{T}_x$  surface ( $\text{f-Ti}_3\text{C}_2\text{T}_x\text{-ZB}$ ).<sup>132</sup> The purpose of amino functionalization of  $\text{Ti}_3\text{C}_2\text{T}_x$  was to improve the dispersion and compatibility of  $\text{Ti}_3\text{C}_2\text{T}_x$  in the epoxy resin matrix. The schematic illustration of the synthesis of  $\text{f-Ti}_3\text{C}_2\text{T}_x\text{-ZB}$  is shown in Fig. 7.

The anti-corrosion and anti-wear performance tests indicated that  $\text{f-Ti}_3\text{C}_2\text{T}_x\text{-ZB@EP}$  composite coating has the best corrosion resistance and better tribological properties in friction-reducing and wear resistance. When the corrosion reactions occur, it would cause a change in pH, causing the BTA in the ZIF-8 nanocontainers to be released. BTA corrosion inhibitors can form corrosion inhibition films on the surface of the metal substrate to further delay the corrosion rate autonomously. The high wear resistance of the  $\text{f-Ti}_3\text{C}_2\text{T}_x\text{-ZB@EP}$  composite coating is mainly due to the lubrication effect of  $\text{f-Ti}_3\text{C}_2\text{T}_x$  and the improvement of plastic deformation resistance. The self-healing function of  $\text{f-Ti}_3\text{C}_2\text{T}_x\text{-ZB}$  creates greater possibilities for the practical application of MXenes in anti-corrosion.

MXenes would be gradually oxidized and degraded in air or water, which would also destroy the integrity of the coatings. Therefore, avoiding the oxidation of MXenes is crucial for the application of MXenes in coatings. Related works were carried out based on this. Ning *et al.* used 1-allyl-3-methylimidazolium

bromide ( $[\text{EMIM}]^+\text{Br}^-$ ) to non-covalently modify MXenes ( $\text{I-Ti}_3\text{C}_2\text{T}_x$ ) to avoid oxidation or deterioration of MXenes.<sup>133</sup> In the antioxidant stability test, after soaking in water for 30 days,  $\text{Ti}_3\text{C}_2\text{T}_x$  dissolved into amorphous  $\text{TiO}_2$  and disordered carbon structures. On the contrary,  $\text{I-Ti}_3\text{C}_2\text{T}_x$  still retained a 2D lamellar structure similar to fresh  $\text{Ti}_3\text{C}_2\text{T}_x$ , which demonstrated that imidazolium salt can effectively delay the degradation of  $\text{Ti}_3\text{C}_2\text{T}_x$  in an aqueous solution. Excellent oxidation resistance plays a vital role in the application of  $\text{Ti}_3\text{C}_2\text{T}_x$  in coatings. Then,  $\text{I-Ti}_3\text{C}_2\text{T}_x$  was dispersed into the epoxy resin matrix to prepare the composite coatings. The corrosion resistance test results showed that when the added amount of  $\text{I-Ti}_3\text{C}_2\text{T}_x$  was 1.0 wt%, the composite coating maintained a high OCP value during the corrosion immersion process, showing better corrosion resistance. After 240 hours of salt spray test, the surface of the 1.0 wt%  $\text{I-Ti}_3\text{C}_2\text{T}_x/\text{EP}$  composite coating remained intact, while the blank EP showed severe corrosion. The Tafel polarization test gave consistent results. 1.0 wt%  $\text{I-Ti}_3\text{C}_2\text{T}_x/\text{EP}$  coating has the lowest corrosion rate ( $1.762 \times 10^{-7}$  mm per year), and the corrosion rate value was lower than other reported coatings. On the one hand, 1-allyl-3-methylimidazolium bromide effectively delayed the oxidative degradation of MXenes so that MXenes can act as stable barriers. On the other hand, the compatibility between MXenes and the epoxy resin matrix was also enhanced. Wu *et al.* used cellulose nanofiber to modify  $\text{Ti}_3\text{C}_2\text{T}_x$  to construct  $\text{Ti}_3\text{C}_2\text{T}_x@\text{CNF}$  nanohybrids and used them as fillers to enhance the corrosion resistance of waterborne epoxy coatings under the marine alternating hydrostatic pressure (AHP) environment.<sup>134</sup> MXene was first etched and then intercalated with dimethyl sulfoxide (DMSO). Then the prepared few-layered delaminated- $\text{Ti}_3\text{C}_2\text{T}_x$  MXenes were mixed with CNF through strong hydrogen bonding forces. The process of MXenes being modified by CNF is shown in Fig. 8a. The corresponding SEM, TEM and SPM results confirmed the success of CNF modification. As a bioadhesive with rich oxygen-containing functional groups, CNF has the ability to enhance the dispersion and compatibility between  $\text{Ti}_3\text{C}_2\text{T}_x$  and epoxy resin, thereby improving the compactness of the composite coatings and also enhancing the adhesion of the epoxy resin to the metal substrates. The excellent adhesion enables the composite coatings to maintain reliable anti-corrosion performance in the harsher deep-sea environment.

Zhao *et al.* prepared antioxidant and high-stability MXene sheets through non-covalent functionalization between MXenes and ionic liquid (IL), and used IL@MXene as smart barrier enhancers for WEP coatings.<sup>135</sup> IL can quench the reactive oxygen species to passivate  $\text{Ti}_3\text{C}_2\text{T}_x$ . In addition, IL has the ability to disperse and stabilize 2D nanomaterials. Tests on the air stability of MXenes inhibited that IL@MXene still retained the complete crystal structures after aging 30 days, but the unmodified MXene sheets have been highly oxidized and destroyed. The electrochemical test results confirmed that the impedance modulus of the IL@MXene-WEP composite coating was increased by 1–2 orders of magnitude compared with the blank WEP coating. This work also confirmed that when MXenes have excellent antioxidant properties, they can exert better corrosion resistance in

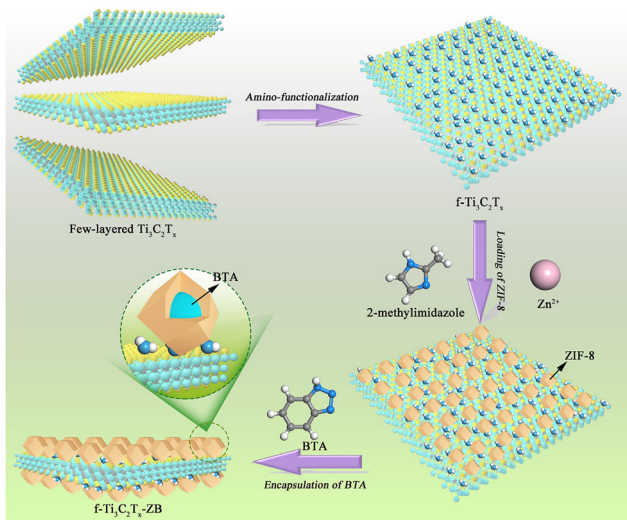


Fig. 7 The synthesis process of  $\text{f-Ti}_3\text{C}_2\text{T}_x\text{-ZB}$ . Reproduced with permission from ref. 132. Copyright 2021 Elsevier.



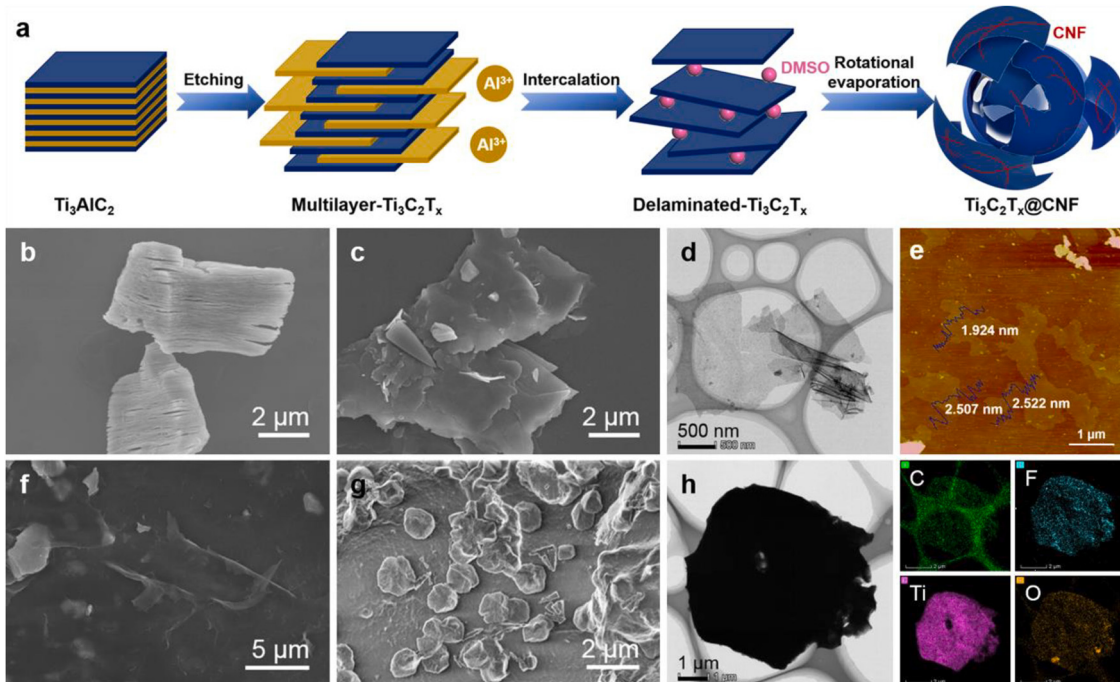


Fig. 8 The process of MXenes being modified by CNF (a); SEM images of (b) multilayer- $\text{Ti}_3\text{C}_2\text{T}_x$  and (c) delaminated- $\text{Ti}_3\text{C}_2\text{T}_x$ ; TEM (d) and SPM (e) images of delaminated- $\text{Ti}_3\text{C}_2\text{T}_x$ ; SEM images of (f)  $\text{Ti}_3\text{C}_2\text{T}_x@\text{CNF}$ , and (g) the cross-sectional image of the  $\text{Ti}_3\text{C}_2\text{T}_x@\text{CNF}$  film; TEM image of (h) the  $\text{Ti}_3\text{C}_2\text{T}_x@\text{CNF}$  topological structure and its elemental mapping. Reproduced with permission from ref. 134. Copyright 2022 Elsevier.

the coatings. In our work, poly(tannic acid) was used to modify the MXene, and zinc ions were introduced at the same time.<sup>136</sup> Through modification, the MXene@PTA-Zn(II) surface contains abundant hydroxyl groups, which increases the compatibility between the fillers and the epoxy coating, greatly enhancing the corrosion resistance.

Some other works combine MXenes with other nanomaterials such as GO, LDHs,  $\text{SiO}_2$ , etc. to achieve synergistic anti-corrosion effects. Relevant experimental results confirm that this synergistic effect is effective in enhancing corrosion resistance. Wu *et al.* prepared the MXene/MgAl-LDH composite film modified with yttrium to improve the corrosion resistance of AZ31 Mg alloy.<sup>137</sup> Since the few-layer MXene sheets have electronegativity and abundant OH groups, they can effectively adsorb  $\text{Mg}^{2+}$  and  $\text{Al}^{3+}$  and provide nucleation sites for the *in situ* growth of LDHs. Therefore, the composite coating layer of MXenes/MgAl-LDH with  $\text{Y(OH)}_3$  can be synthesized on the AZ31 Mg alloy surface through a one-step hydrothermally chemical conversion method. MXenes can effectively cover the cracks in the LDH coatings to better prevent the penetration of corrosive media. LDHs can further inhibit corrosion through the anion exchange. Furthermore,  $\text{Y(OH)}_3$  as a corrosion inhibitor can enable active anti-corrosion of the composite coatings. Cai *et al.* also prepared the composite of MXenes and LDHs and used the composite materials to enhance the corrosion resistance and friction resistance of epoxy resin coatings.<sup>138</sup> DFT calculations indicated that the heterostructure of  $\text{Ti}_3\text{C}_2\text{T}_x$  MXene and MgAl-LDH has strong binding stability, and  $\text{Ti}_3\text{C}_2\text{T}_x$  MXene@MgAl-LDH still has great dispersion and compatibility with epoxy

resin after standing for 160 days. Shen *et al.* grafted MXenes on the surface of GO nanosheets through nucleophilic substitution and used the composite materials to improve the corrosion resistance of epoxy zinc-rich coatings.<sup>139</sup> The high conductivity  $\text{Ti}_3\text{C}_2$  in GO- $\text{Ti}_3\text{C}_2$  can enhance the electrical connection between Zn particles and the steel matrix, providing a new conductive path between the zinc particles and the steel matrix, so that the zinc-rich coatings improve the utilization of zinc particles. In addition, GO can exert an excellent shielding effect on corrosive media. OCP, EIS and salt spray test results all confirmed that GO- $\text{Ti}_3\text{C}_2$  improved the cathodic protection ability of epoxy zinc-rich coatings, which provides new inspiration for the enhancement of corrosion resistance of epoxy zinc-rich coatings.  $\text{TiO}_2$  can also be used to modify MXenes. When 0.1%  $\text{Ti}_3\text{C}_2$ & $\text{TiO}_2$  was incorporated into the waterborne polyurethane coating, the corrosion resistance of coatings was significantly improved.  $\text{Ti}_3\text{C}_2$  and  $\text{TiO}_2$  repaired micropores and cracks in coatings while also enhancing the hydrophobicity of the waterborne polyurethane coating.<sup>140</sup>

We prepared polydopamine (PDA) modified MXene-ZrP composites using a one-pot method and applied the MXene-ZrP@PDA (MZP) heterojunction to enhance the corrosion and wear resistance of waterborne epoxy coatings.<sup>141</sup> The corrosion test results indicated that the corrosion rate of the MZP/WEP composite coating was reduced by an order of magnitude compared with the blank WEP coating. The two-dimensional nanosheet materials can extend the diffusion path of the corrosion media. In addition, combining ZrP and MXene effectively improves the aggregation effect of MXenes. The surface



modification of PDA improves the interfacial compatibility of MZP in epoxy resin. Furthermore, PDA can capture  $\text{Fe}^{3+}$  and form  $\text{Fe}^{3+}$ -PDA complexes to further delay the occurrence of corrosion. MZP composite materials also effectively improve the wear resistance of the MZP/WEP coating. Its average coefficient of friction (COF) was reduced by 82.06% compared with the blank WEP coating. We also grew structurally stable alkoxy silane modified  $\text{SiO}_2$  *in situ* on the MXene's surface to prepare a 0D/2D nanohybrid ( $\text{FSiO}_2$ -MX).<sup>142</sup> The insulating  $\text{FSiO}_2$  would reduce the current effect of MXenes, thus inhibiting the occurrence of galvanic corrosion. In addition, the amino groups on the surface of  $\text{SiO}_2$  react with the epoxy resin to further promote resin curing and reduce defects in the WEP coating.

Some other green corrosion inhibitors can also be applied to modify MXenes and achieve better corrosion prevention. L-Cysteine is widely used as a green corrosion inhibitor. Li *et al.* applied L-cysteine as a surface modifier for MXenes (fMX) to enhance the dispersion performance of MXenes in the epoxy matrix (shown in Fig. 9).<sup>143</sup>

The electrochemical test results indicated that the corrosion rate of the fMX composite coating was reduced by 3 orders of magnitude compared with the blank waterborne epoxy coating. fMX nanosheets have great dispersion in the epoxy matrix. In addition, there is a strong interfacial interaction between fMX and epoxy groups, which delayed the diffusion of corrosive media and improved the corrosion resistance of the waterborne epoxy coating. Chitosan is the product of removing some of the acetyl groups from the natural polysaccharide chitin and is an environmentally friendly green corrosion inhibitor. Our strategy was to apply phosphorylated chitosan to functionally modify MXenes and use the modified MXene as a filler for waterborne epoxy coatings, which can effectively inhibit the galvanic corrosion of MXenes.<sup>144</sup> The combination of chitosan and MXenes can achieve a good synergistic effect. The agglomeration tendency of MXenes was eliminated, and chitosan can also play a corrosion inhibition role. Moreover, the

adhesion between the coatings and the substrate was also increased, which further enhanced the corrosion resistance of the WEP coatings. Silk fibroin can also be used to modify MXenes, the protein fibers on the surface of SF-MXene nanosheets were beneficial to the interface with the resin improving the mechanical properties of the coating. SF- $\text{Ti}_3\text{C}_2\text{T}_x$ /epoxy composite coatings exhibit excellent protection and delayed failure capabilities in harsh deep-sea environments.<sup>145</sup> Sheng *et al.* reported that MXene is also a great phosphating accelerator that can effectively improve the corrosion resistance of the phosphate coating.<sup>146,147</sup> In addition, MXenes have also shown promise for preparing functional polymers with superior flame retardancy and smoke suppression ability.

### 3.3. Applications of TMDs in corrosion prevention

Daniel S. Schulman *et al.* discovered that single-layer transition metal dichalcogenides have high resistance to electro-oxidation and corrosion.<sup>148</sup> This is due to the excellent chemical stability of monomolecular delamination in oxidative corrosion environments, which indicates that TMD materials, especially disulfides, have great prospects and potential economic impact in anti-corrosion applications. Among TMDs, layered molybdenum disulfide ( $\text{MoS}_2$ ) has attracted increasing attention in the field of anti-corrosion due to its special hydrophobicity, ultra-thin atomic layer structure, and large specific surface area. Although exposed  $\text{MoS}_2$  is easily corroded and oxidized, when it is added as the nanofiller to the polymer coatings, the corrosion resistance of the prepared nanocomposite coatings can be increased. Ding *et al.* prepared layered TMD nanosheets of  $\text{MoS}_2$  and  $\text{WS}_2$  through liquid exfoliation technology, and incorporated these two nanosheets into the epoxy matrix.<sup>149</sup> The electrochemical test results fully confirmed that the low conductivity of TMDs can effectively cut off the electronic path of microgalvanic corrosion and inhibit the occurrence of corrosion. There have been some reports that using other substances to modify  $\text{MoS}_2$  to prepare composite polymer coatings can effectively extend the life of the polymer coatings. Xia *et al.* used PDA to modify  $\text{MoS}_2$  and  $\text{PDA}@\text{MoS}_2$  to improve the corrosion

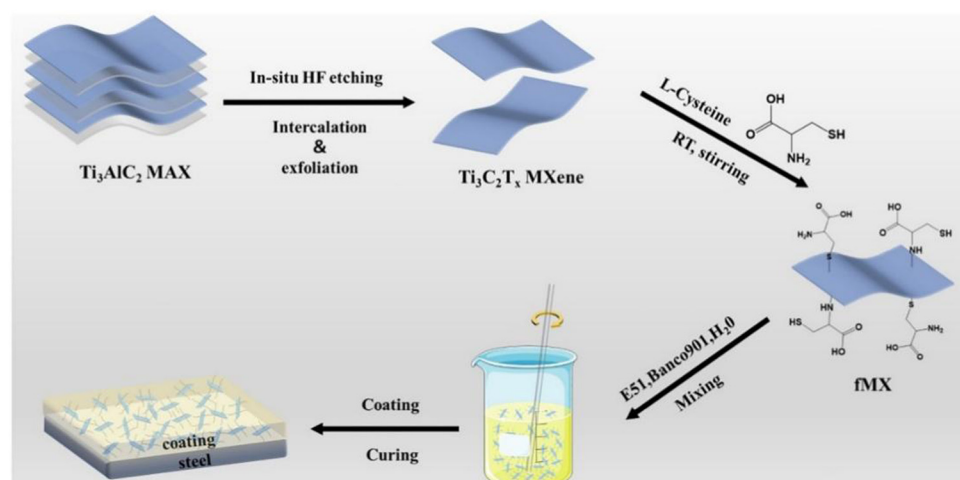


Fig. 9 The preparation process of MXene ( $\text{Ti}_3\text{C}_2\text{T}_x$ ), fMX and the composite coating. Reproduced with permission from ref. 143. Copyright 2021 Elsevier.



resistance of epoxy resin.<sup>150</sup> Compared with the blank EP coating, the corrosion resistance of the composite  $\text{MoS}_2$ @PDA/EP coating was greatly enhanced. In addition, the adhesion strength of the epoxy coating to the metal matrix has also been enhanced by about 3 MPa. Zhao *et al.* used sodium dodecyl benzene sulfonate to modify  $\text{MoS}_2$  and fabricated a 2D  $\text{MoS}_2$ /SDBS composite coating on carbon steel.<sup>151</sup>  $\text{MoS}_2$ /SDBS can effectively fill the voids of an epoxy coating to increase corrosion resistance. Gao *et al.* successfully prepared  $\text{MoS}_2$ /acrylic composite coatings on the surface of galvanized sheets.<sup>152</sup> Tannic acid and hydroxyethylidene diphosphonic acid were also added. The addition of  $\text{MoS}_2$  effectively reduced the corrosion rate and corrosion current density of acrylic coatings. Jing *et al.* applied gamma-(2,3-epoxypropoxy) propyltrimethoxy silane (KH560) to modify  $\text{MoS}_2$ .<sup>153</sup> The silane coupling agent can act as an intermediate bridge to increase the compatibility and interfacial force between the nanofiller and coatings. When 0.8 wt% KH560- $\text{MoS}_2$  was incorporated, the corrosion resistance of epoxy coatings was significantly enhanced. Similarly, other two-dimensional sheet materials combined with TMDs can also achieve

synergistic anti-corrosion effects. H-BN was added to  $\text{MoS}_2$  and deposited on the surface of mild steel. Compared with pure  $\text{MoS}_2$  coating, the corrosion resistance of the  $\text{MoS}_2$ -hBN coating was enhanced and the corrosion rate was significantly reduced.<sup>154</sup> Chen *et al.* uniformly loaded  $\text{MoS}_2$  on the surface of graphene oxide, and then modified  $\text{MoS}_2$ -RGO with KH560 to improve the dispersion stability of  $\text{MoS}_2$ -RGO in the polymer coatings.<sup>155</sup> In this work,  $\text{MoS}_2$  and RGO achieved a synergistic anti-corrosion effect. Their excellent shielding effect greatly increased the penetration resistance of coatings.

Although TMDs can effectively extend the thermal stability, toughness and mechanical properties of the coatings, the physical barrier alone cannot protect the coatings for a long time, and once the coatings are damaged, the damage is irreversible.

Milad Motamedi *et al.* proposed a strategy of encapsulating corrosion inhibitors Pr and tannate into ZIF8 anchored on the surface of  $\text{MoS}_2$  to achieve smart anti-corrosion of the coatings.<sup>156</sup> EP/Pr-TA-ZIF8@MS composite coatings can control

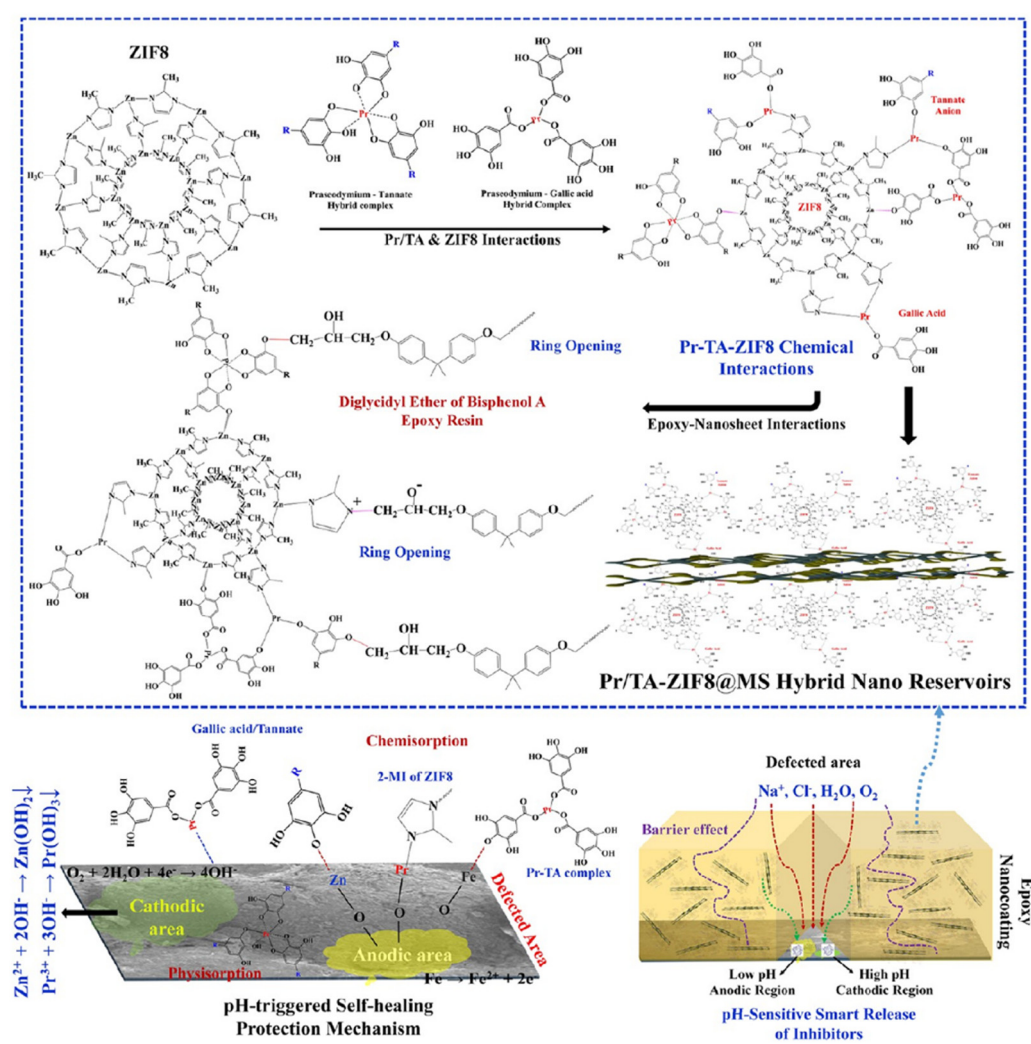


Fig. 10 The self-healing protection mechanism of the EP/Pr-TA-ZIF8@MS nanocoating. Reproduced with permission from ref. 156. Copyright 2022 American Chemical Society.

the release of corrosion inhibitors through changes in pH to achieve anti-corrosion. The self-healing protection mechanism of the EP/Pr-TA-ZIF8@MS nanocoating is shown in Fig. 10.

Firstly, the nanosheet materials dispersed in the polymer coatings can enhance the curvature of the diffusion paths of oxygen and water in the epoxy coatings, allowing the EP/Pr-TA-ZIF8@MS composite coatings to have an excellent barrier function. Secondly, as the pH changes, the effective inorganic cations and organic molecules in the nanocontainer would be released to the sensitive active sites of the metal, forming a corrosion inhibition layer adsorbed on the surface of the metal matrix to delay the occurrence of corrosion reactions.  $\text{Pr}^{3+}/\text{Zn}^{2+}$  and tannate/2-MI in the nano reservoir would be intelligently released to the low pH anode and high pH cathode of the metal matrix at the same time by pH-triggered framework hydrolysis and ion/ligand exchange activities. Hence, adhesion-stabilizing complexes of Pr/Zn-tannate, Pr/Zn-tannate-Fe, and Pr/Zn-MI-Fe adherent/stable complexes are formed at the damaged part of the metal substrate. In addition, the adhesion loss of the EP/Pr-TA-ZIF8@MS nanocomposite coating was reduced by 71.1%, and cathodic debonding was effectively reduced by 60.11%. Compared with the blank EP, the cross-linking density and tensile strength of the EP/Pr-TA-ZIF8@MS composite coating were significantly enhanced. This is an impressive strategy that provides new ideas for the use of nanomaterials in composite coatings and the controlled release of corrosion inhibitors.

## 4. Summary

### 4.1. Concluding remarks

This article briefly introduces the structure and properties of two-dimensional transition metal layered materials including LDHs, TMDs and MXenes and their applications in metal corrosion prevention. Due to the two-dimensional lamellar structures and excellent physical and chemical properties, LDHs, MXenes and TMDs have great application prospects in the field of metal anti-corrosion. The conclusions are summarized as follows:

1. LDHs can not only act as nanofillers in polymer coatings, but also form chemical conversion coatings to protect metal substrates from corrosion damage.

2. TMDs and MXenes are easily oxidized, corrosion prevention is not obvious when TMDs and MXenes are directly introduced into polymer coatings. Therefore, it is necessary to functionalize two-dimensional transition metal layered materials before introducing them into polymer coatings.

3. Modification can also solve the problem of easy agglomeration of two-dimensional transition metal layered materials in polymer coatings.

4. A lot of research works have confirmed that two-dimensional transition metal layered materials contribute to increasing the corrosion resistance of coatings.

### 4.2. Outlook

Although existing works have confirmed that two-dimensional transition metal nanomaterials have great permeability

resistance and can enhance the corrosion resistance of nanocomposite coatings, there are still some problems that need to be improved. In the future, the application of two-dimensional transition metal nanomaterials in metal corrosion prevention can consider making breakthroughs in the following aspects:

1. Two-dimensional transition metal nanomaterials, especially TMDs and MXenes, are easily oxidized, which is extremely detrimental to the performance of the subsequent constructed nanocomposite coatings. Future research should continue to focus on solving this problem to ensure the stability of the two-dimensional transition metal nanomaterials.

2. Single-function coatings can no longer meet the needs of social development. It must be considered that the coatings should exhibit more functions, such as self-healing, superhydrophobic, friction resistance, flame retardant, etc., when two-dimensional transition metal nanomaterials are introduced.

3. The corrosion data of two-dimensional transition metal material nanocomposite coatings in actual application scenarios should be tested and the corrosion data should be monitored in real time.

4. Appropriate models should be established to predict the corrosion process of two-dimensional transition metal material nanocomposite coatings in a more intelligent way.

## Conflicts of interest

The authors declare no competing financial interest.

## Acknowledgements

This work was supported by the Centrally Guided Local Science and Technology Development Fund Project (Grant No. 22ZY1QA011); the Hongliu Outstanding Young Talent Support Program of Lanzhou University of Technology; and the Lanzhou Talent Innovation and Entrepreneurship Project (Grant No. 2023-RC-46).

## References

- 1 K. S. Novoselov, A. K. Geim, S. V. Morozov, D. Jiang, Y. Zhang, S. V. Dubonos, I. V. Grigorieva and A. A. Firsov, *Science*, 2004, **306**, 666–669.
- 2 F. Zhou, Y. Ma, Y. Chen, L. Zhang and X. Sheng, *Prog. Org. Coat.*, 2024, **186**, 108007.
- 3 D. Huang, L. Zhang, X. Sheng and Y. Chen, *Appl. Therm. Eng.*, 2023, **232**, 121041.
- 4 R. Lv, J. A. Robinson, R. E. Schaak, D. Sun, Y. Sun, T. E. Mallouk and M. Terrones, *Acc. Chem. Res.*, 2015, **48**, 56–64.
- 5 G. Mishra, B. Dash and S. Pandey, *Appl. Clay Sci.*, 2018, **153**, 172–186.
- 6 X.-J. Zhao, S.-M. Xu, P. Yin, J.-Y. Guo, W. Zhang, Y. Jie and H. Yan, *Chem. Eng. J.*, 2023, **451**, 138500.



7 M. A. Nazir, T. Najam, S. Jabeen, M. A. Wattoo, M. S. Bashir, S. S. A. Shah and A. U. Rehman, *Inorg. Chem. Commun.*, 2022, **145**, 110008.

8 M. Chhowalla, H. S. Shin, G. Eda, L.-J. Li, K. P. Loh and H. Zhang, *Nat. Chem.*, 2013, **5**, 263–275.

9 X. Zhang, X.-F. Qiao, W. Shi, J.-B. Wu, D.-S. Jiang and P.-H. Tan, *Chem. Soc. Rev.*, 2015, **44**, 2757–2785.

10 Y. Shen, L. Liang, S. Zhang, D. Huang, J. Zhang, S. Xu, C. Liang and W. Xu, *Nanoscale*, 2018, **10**, 1622–1630.

11 E. Lee, Y. S. Yoon and D.-J. Kim, *ACS Sens.*, 2018, **3**, 2045–2060.

12 S. Alwarappan, N. Nesakumar, D. Sun, T. Y. Hu and C.-Z. Li, *Biosens. Bioelectron.*, 2022, **205**, 113943.

13 X. Guan, Z. Yang, M. Zhou, L. Yang, R. Peymanfar, B. Aslubeiki and G. Ji, *Small Struct.*, 2022, **3**, 2200102.

14 J. Jiang, S. Bai, J. Zou, S. Liu, J.-P. Hsu, N. Li, G. Zhu, Z. Zhuang, Q. Kang and Y. Zhang, *Nano Res.*, 2022, **15**, 6551–6567.

15 A. Iqbal, T. Hassan, Z. Gao, F. Shahzad and C. M. Koo, *Carbon*, 2023, **203**, 542–560.

16 J. Li, F. Meng, L. Liu, Y. Cui, R. Liu, H. Zheng and F. Wang, *Corros. Commun.*, 2022, **5**, 62–72.

17 X. Huang, Q. Weng, Y. Chen, L. Zhang and X. Sheng, *Surf. Interfaces*, 2024, **45**, 103911.

18 J. Shen, Y. Ma, F. Zhou, X. Sheng and Y. Chen, *J. Mater. Sci. Technol.*, 2024, DOI: [10.1016/j.jmst.2024.01.014](https://doi.org/10.1016/j.jmst.2024.01.014).

19 T. Liu, L. Ma, X. Wang, J. Wang, H. Qian, D. Zhang and X. Li, *Corros. Commun.*, 2021, **1**, 18–25.

20 Y. Tian, H. Huang, H. Wang, Y. Xie, X. Sheng, L. Zhong and X. Zhang, *J. Alloys Compd.*, 2020, **831**, 154906.

21 Y. Tian, L. Zhong, X. Sheng and X. Zhang, *Adv. Compos. Hybrid Mater.*, 2022, **5**, 1922–1938.

22 S. Nahirniak, A. Ray and B. Saruhan, *Batteries*, 2023, **9**, 126.

23 Y. Wang, T. Guo, Z. Tian, K. Bibi, Y. Zhang and H. N. Alshareef, *Adv. Mater.*, 2022, **34**, 2108560.

24 M. S. Javed, A. Mateen, S. Ali, X. Zhang, I. Hussain, M. Imran, S. S. A. Shah and W. Han, *Small*, 2022, **18**, 2201989.

25 K. Li, J. Li, Q. Zhu and B. Xu, *Small Methods*, 2022, **6**, 2101537.

26 Q. Fu, J. Han, X. Wang, P. Xu, T. Yao, J. Zhong, W. Zhong, S. Liu, T. Gao, Z. Zhang, L. Xu and B. Song, *Adv. Mater.*, 2021, **33**, 1907818.

27 M. Xu and M. Wei, *Adv. Funct. Mater.*, 2018, **28**, 1802943.

28 H. Yi, S. Liu, C. Lai, G. Zeng, M. Li, X. Liu, B. Li, X. Huo, L. Qin, L. Li, M. Zhang, Y. Fu, Z. An and L. Chen, *Adv. Energy Mater.*, 2021, **11**, 2002863.

29 Z. Bi, R. Guo, X. Hu, J. Wang, X. Chen and W. Pan, *Nanoscale*, 2022, **14**, 3367–3386.

30 T. Hu, Z. Gu, G. R. Williams, M. Strimaitė, J. Zha, Z. Zhou, X. Zhang, C. Tan and R. Liang, *Chem. Soc. Rev.*, 2022, **51**, 6126–6176.

31 A. K. Mia, M. Meyyappan and P. K. Giri, *Biosensors*, 2023, **13**, 169.

32 D. S. Schulman, D. May-Rawding, F. Zhang, D. Buzzell, N. Alem and S. Das, *ACS Appl. Mater. Interfaces*, 2018, **10**, 4285–4294.

33 L. Ma, Y. Qiang and W. Zhao, *Chem. Eng. J.*, 2021, **408**, 127367.

34 H. Jiang, Y. Xie, R. Zhu, Y. Luo, X. Sheng, D. Xie and Y. Mei, *Chem. Eng. J.*, 2023, **456**, 141049.

35 Y. Luo, Y. Xie, W. Geng, J. Chu, H. Wu, D. Xie, X. Sheng and Y. Mei, *J. Mater. Sci. Technol.*, 2022, **129**, 27–39.

36 Y. Cao, M. Weng, M. H. H. Mahmoud, A. Y. Elnaggar, L. Zhang, I. H. El Azab, Y. Chen, M. Huang, J. Huang and X. Sheng, *Adv. Compos. Hybrid Mater.*, 2022, **5**, 1253–1267.

37 Z. Gu, J. J. Atherton and Z. P. Xu, *Chem. Commun.*, 2015, **51**, 3024–3036.

38 J. Yu, Q. Wang, D. O'Hare and L. Sun, *Chem. Soc. Rev.*, 2017, **46**, 5950–5974.

39 X. Zhang, Y. Zhang, Y. Lv, Z. Dong, T. Hashimoto and X. Zhou, *Corros. Commun.*, 2022, **6**, 67–83.

40 V. Zahedi Asl, J. Zhao, Y. Palizdar and M. Junaid Anjum, *Corros. Commun.*, 2022, **5**, 73–86.

41 J. Li, F. Meng, L. Liu, Y. Cui, R. Liu, H. Zheng and F. Wang, *Corros. Commun.*, 2022, **5**, 62–72.

42 A. Jagtap, P. G. Wagle, E. Jagtiani and A. P. More, *J. Coat. Technol. Res.*, 2022, **19**, 1009–1032.

43 A. V. Karim, A. Hassani, P. Eghbali and P. V. Nidheesh, *Curr. Opin. Solid State Mater. Sci.*, 2022, **26**, 100965.

44 H. N. Tran, D. T. Nguyen, G. T. Le, F. Tomul, E. C. Lima, S. H. Woo, A. K. Sarmah, H. Q. Nguyen, P. T. Nguyen, D. D. Nguyen, T. V. Nguyen, S. Vigneswaran, D.-V. N. Vo and H.-P. Chao, *J. Hazard. Mater.*, 2019, **373**, 258–270.

45 R. M. M. Santos, J. Tronto, V. Briois and C. V. Santilli, *J. Mater. Chem. A*, 2017, **5**, 9998–10009.

46 L. Liu, Q. Deng, P. White, S. Dong, I. S. Cole, J. Dong and X.-B. Chen, *Corros. Commun.*, 2022, **8**, 40–48.

47 M. Zubair, I. Ihsanullah, H. Abdul Aziz, M. Azmier Ahmad and M. A. Al-Harthi, *Bioresour. Technol.*, 2021, **319**, 124128.

48 L. Mohapatra and K. Parida, *J. Mater. Chem. A*, 2016, **4**, 10744–10766.

49 V. K. Ameena Shirin, R. Sankar, A. P. Johnson, H. V. Gangadharappa and K. Pramod, *J. Controlled Release*, 2021, **330**, 398–426.

50 W. Feitknecht, *Helv. Chim. Acta*, 1942, **25**, 555–569.

51 M. A. Aramendia, Y. Avilés, V. Borau, J. M. Luque, J. M. Marinas, J. R. Ruiz and F. J. Urbano, *J. Mater. Chem.*, 1999, **9**, 1603–1607.

52 F. Thevenot, R. Szymanski and P. Chaumette, *Clays Clay Miner.*, 1989, **37**, 396–402.

53 M. Ogawa and H. Kaiho, *Langmuir*, 2002, **18**, 4240–4242.

54 A. V. Radha, P. Vishnu Kamath and C. Shivakumara, *Solid State Sci.*, 2005, **7**, 1180–1187.

55 M. Meyn, K. Beneke and G. Lagaly, *Inorg. Chem.*, 1993, **32**, 1209–1215.

56 F. Wong and R. G. Buchheit, *Prog. Org. Coat.*, 2004, **51**, 91–102.

57 W. Li, J. Lu, J. Chen, G. Li, Y. Jiang, L. Li and B. Huang, *J. Chem. Technol. Biotechnol.*, 2006, **81**, 89–93.

58 M. Naguib, M. Kurtoglu, V. Presser, J. Lu, J. Niu, M. Heon, L. Hultman, Y. Gogotsi and M. W. Barsoum, *Adv. Mater.*, 2011, **23**, 4248–4253.



59 J. Pang, B. Chang, H. Liu and W. Zhou, *ACS Energy Lett.*, 2022, **7**, 78–96.

60 Z. Othman, H. R. Mackey and K. A. Mahmoud, *Chemosphere*, 2022, **295**, 133849.

61 M. Naguib, V. N. Mochalin, M. W. Barsoum and Y. Gogotsi, *Adv. Mater.*, 2014, **26**, 992–1005.

62 X. Meng, L. Wang, X. Wang, M. Zhen, Z. Hu, S.-Q. Guo and B. Shen, *Chemosphere*, 2023, **338**, 139550.

63 K. Gong, Y. Peng, A. Liu, S. Qi and H. Qiu, *Composites, Part A*, 2024, **176**, 107857.

64 X. He, J. Wu, X. Huang, Y. Chen, L. Zhang and X. Sheng, *Chem. Eng. Sci.*, 2024, **283**, 119429.

65 J. Wu, Y. Chen, L. Zhang and X. Sheng, *J. Ind. Eng. Chem.*, 2024, **129**, 424–434.

66 Y. Li, S. Huang, S. Peng, H. Jia, J. Pang, B. Ibarlucea, C. Hou, Y. Cao, W. Zhou, H. Liu and G. Cuniberti, *Small*, 2023, **19**, 2206126.

67 X. He, J. Wu, X. Huang, Y. Chen, L. Zhang and X. Sheng, *Chem. Eng. Sci.*, 2024, **283**, 119429.

68 M. AhadiParsa, A. Dehghani, M. Ramezanzadeh and B. Ramezanzadeh, *Adv. Colloid Interface Sci.*, 2022, **307**, 102730.

69 S. Sharma, A. Kumar and E. E. Ebenso, *Mater. Lett.*, 2023, **335**, 133789.

70 X. Hu, B. Quan, C. Zhu, H. Wen, M. Sheng, S. Liu, X. Li, H. Wu, X. Lu and J. Qu, *Adv. Sci.*, 2023, **10**, 2206835.

71 D. Huang, Y. Chen, L. Zhang and X. Sheng, *J. Mater. Sci. Technol.*, 2023, **165**, 27–38.

72 M. Naguib, M. Kurtoglu, V. Presser, J. Lu, J. Niu, M. Heon, L. Hultman, Y. Gogotsi and M. W. Barsoum, *Adv. Mater.*, 2011, **23**, 4248–4253.

73 M. Ghidiu, M. R. Lukatskaya, M.-Q. Zhao, Y. Gogotsi and M. W. Barsoum, *Nature*, 2014, **516**, 78–81.

74 P. Urbankowski, B. Anasori, T. Makaryan, D. Er, S. Kota, P. L. Walsh, M. Zhao, V. B. Shenoy, M. W. Barsoum and Y. Gogotsi, *Nanoscale*, 2016, **8**, 11385–11391.

75 T. Li, L. Yao, Q. Liu, J. Gu, R. Luo, J. Li, X. Yan, W. Wang, P. Liu, B. Chen, W. Zhang, W. Abbas, R. Naz and D. Zhang, *Angew. Chem.*, 2018, **130**, 6223–6227.

76 S. Yang, P. Zhang, F. Wang, A. G. Ricciardulli, M. R. Lohe, P. W. M. Blom and X. Feng, *Angew. Chem., Int. Ed.*, 2018, **57**, 15491–15495.

77 X. Yin, C. S. Tang, Y. Zheng, J. Gao, J. Wu, H. Zhang, M. Chhowalla, W. Chen and A. T. S. Wee, *Chem. Soc. Rev.*, 2021, **50**, 10087–10115.

78 J. Radhakrishnan, S. Ratna and K. Biswas, *Inorg. Chem. Commun.*, 2022, **145**, 109971.

79 R. F. Frindt and A. D. Yoffe, *Proc. R. Soc. Lond. A*, 1963, **273**, 69–83.

80 S. Aftab and H. H. Hegazy, *Small*, 2023, **19**, 2205778.

81 A. Alfieri, S. B. Anantharaman, H. Zhang and D. Jariwala, *Adv. Mater.*, 2023, **35**, 2109621.

82 S. Ali, S. S. Ahmad Shah, M. Sufyan Javed, T. Najam, A. Parkash, S. Khan, M. A. Bajaber, S. M. M. Eldin, R. A. Tayeb, M. M. Rahman and J. Qi, *Chem. Rec.*, 2023, e202300145.

83 A. Joseph, A. S. Vijayan, C. M. Shebeeb, K. S. Akshay, K. P. John Mathew and V. Sajith, *J. Mater. Chem. A*, 2023, **11**, 3172–3209.

84 R. Yang, Y. Fan, Y. Zhang, L. Mei, R. Zhu, J. Qin, J. Hu, Z. Chen, Y. Hau Ng, D. Voiry, S. Li, Q. Lu, Q. Wang, J. C. Yu and Z. Zeng, *Angew. Chem., Int. Ed.*, 2023, **62**, e202218016.

85 Y. Shi, B. Yang and P. Liaw, *Metals*, 2017, **7**, 43.

86 Y. Tian, Y. Xie, F. Dai, H. Huang, L. Zhong and X. Zhang, *Surf. Coat. Technol.*, 2020, **383**, 125227.

87 Y. Tian, W. Qiu, Y. Xie, H. Huang, J. Hu, L. Zhong, X. Jiang and X. Zhang, *J. Electrochem. Soc.*, 2020, **167**, 101505.

88 C. M. Hansson, *Metall. Mater. Trans. A*, 2011, **42**, 2952–2962.

89 L. M. Zhang, S. D. Zhang, A. L. Ma, H. X. Hu, Y. G. Zheng, B. J. Yang and J. Q. Wang, *Corros. Sci.*, 2018, **144**, 172–183.

90 A. Fateh, M. Aliofkhazraei and A. R. Rezvanian, *Arabian J. Chem.*, 2020, **13**, 481–544.

91 N. K. Prasad, A. S. Pathak, S. Kundu and K. Mondal, *Corros. Sci.*, 2021, **189**, 109616.

92 T. Vu Dinh, W. W. Sun, Y. Yue, Y. Wu, C. R. Hutchinson and S. Thomas, *Corros. Sci.*, 2018, **145**, 67–79.

93 S. Kumar, T. Banerjee and D. Patel, *Mater. Today: Proc.*, 2020, **33**, 5678–5682.

94 L. A. Hernández-Alvarado, L. S. Hernández, J. Garrido, S. Rivera-Villalobos and M. L. Escudero, *Surf. Coat. Technol.*, 2017, **325**, 473–481.

95 H. Xu and Y. Zhang, *Coatings*, 2019, **9**, 807.

96 Y. Tian, W. Wang, L. Zhong, X. Jiang and X. Zhang, *Prog. Org. Coat.*, 2022, **163**, 106655.

97 D. Zhang, F. Peng and X. Liu, *J. Alloys Compd.*, 2021, **853**, 157010.

98 X. Zhang, F. Zhong, X. Li, B. Liu, C. Zhang, B. Buhe, T. Zhang, G. Meng and F. Wang, *J. Alloys Compd.*, 2019, **788**, 756–767.

99 X. Guo, F. Zhang, D. G. Evans and X. Duan, *Chem. Commun.*, 2010, **46**, 5197.

100 L. Guo, W. Wu, Y. Zhou, F. Zhang, R. Zeng and J. Zeng, *J. Mater. Sci. Technol.*, 2018, **34**, 1455–1466.

101 A. C. Bouali, M. H. Iuzviuk, M. Serdechnova, K. A. Yasakau, D. Drozdenko, A. Lutz, K. Fekete, G. Dovzhenko, D. C. F. Wieland, H. Terryn, M. G. S. Ferreira, I. A. Zobkalo and M. L. Zheludkevich, *J. Phys. Chem. C*, 2021, **125**, 11687–11701.

102 M. J. Anjum, J. Zhao, V. Zahedi Asl, G. Yasin, W. Wang, S. Wei, Z. Zhao and W. Qamar Khan, *Corros. Sci.*, 2019, **157**, 1–10.

103 Y. Zhang, J. Liu, Y. Li, M. Yu, S. Li and B. Xue, *J. Coat. Technol. Res.*, 2015, **12**, 595–601.

104 K. Lin, X. Luo, X. Pan, C. Zhang and Y. Liu, *Appl. Surf. Sci.*, 2019, **463**, 1085–1096.

105 Y. Cao, D. Zheng, X. Li, J. Lin, C. Wang, S. Dong and C. Lin, *ACS Appl. Mater. Interfaces*, 2018, **10**, 15150–15162.

106 C. Zhang, X. Luo, X. Pan, L. Liao, X. Wu and Y. Liu, *Appl. Surf. Sci.*, 2017, **394**, 275–281.

107 I. Mohammadi, T. Shahrebi, M. Mahdavian and M. Izadi, *Surf. Coat. Technol.*, 2021, **409**, 126882.



108 H. Wang, Y. Song, X. Chen, G. Tong and L. Zhang, *Corros. Sci.*, 2022, **208**, 110699.

109 W. Jian, Z. Jin, J. Yang, G. Meng, H. Liu and H. Liu, *J. Ind. Eng. Chem.*, 2022, **113**, 419–430.

110 D. Li, X. Cui, X. Wen, Y. Li, E. Liu, G. Jin and W. Zheng, *J. Alloys Compd.*, 2023, **947**, 169666.

111 Y. Jiang, S. Gao, Y. Liu, H. Huangfu, X. Guo and J. Zhang, *Surf. Coat. Technol.*, 2022, **440**, 128504.

112 N. Huang, Y. Wang, Y. Zhang, L. Liu, N. Yuan and J. Ding, *Surf. Coat. Technol.*, 2023, **463**, 129539.

113 X. Dai, L. Wu, W. Ci, W. Yao, Y. Yuan, Z. Xie, B. Jiang, J. Wang, A. Andrej and F. Pan, *Corros. Sci.*, 2023, **220**, 111285.

114 Y. Chen, L. Wu, W. Yao, J. Wu, Y. Yuan, Z. Xie, B. Jiang and F. Pan, *Colloids Surf., A*, 2022, **655**, 130339.

115 Y. Wu, L. Wu, W. Yao, B. Jiang, J. Wu, Y. Chen, X. Chen, Q. Zhan, G. Zhang and F. Pan, *Electrochim. Acta*, 2021, **374**, 137913.

116 Y. Chen, L. Wu, W. Yao, J. Wu, J. Xiang, X. Dai, T. Wu, Y. Yuan, J. Wang, B. Jiang and F. Pan, *J. Mater. Sci. Technol.*, 2022, **130**, 12–26.

117 N. S. Sangaj and V. C. Malshe, *Prog. Org. Coat.*, 2004, **50**, 28–39.

118 N. Sharma and S. Sharma, *Mater. Today: Proc.*, 2021, **44**, 4498–4502.

119 H. Xu and Y. Zhang, *Coatings*, 2019, **9**, 807.

120 C. Liu, S. Qiu, P. Du, H. Zhao and L. Wang, *Nanoscale*, 2018, **10**, 8115–8124.

121 M. Zhang, F. Xu, D. Lin, J. Peng, Y. Zhu and H. Wang, *Chem. Eng. J.*, 2022, **446**, 137078.

122 N. Wang, H. Gao, J. Zhang, L. Li, X. Fan and X. Diao, *Prog. Org. Coat.*, 2019, **135**, 74–81.

123 T. Xu, Y. Zhao, J.-H. Zhou and J.-M. Hu, *Prog. Org. Coat.*, 2022, **164**, 106695.

124 C. B. Pawar, P. D. Desai, H. N. Bagde and A. P. More, *Arab. J. Sci. Eng.*, 2023, **48**, 7739–7753.

125 C. Ding, J. Wu, Y. Liu, X. Sheng, X. Cheng, X. Xiong and W. Zhao, *Molecules*, 2023, **28**, 5199.

126 H. Jiang, Y. Xie, Y. Jiang, Y. Luo, X. Sheng, Y. Mei and D. Xie, *Appl. Surf. Sci.*, 2024, **649**, 159111.

127 J. Ding, H. Zhao and H. Yu, *Chem. Eng. J.*, 2022, **430**, 132838.

128 H. Cao, M. Fang, W. Jia, X. Liu and Q. Xu, *Composites, Part B*, 2022, **228**, 109427.

129 A. Sadanandan, S. A. Thomas, M. E. Khan, M. S. Alomar, M. R. Pallavolu and J. Cherusseri, *Prog. Org. Coat.*, 2023, **183**, 107757.

130 X. Sun, C. Ma, F. Ma, T. Wang, C. Feng and W. Wang, *J. Alloys Compd.*, 2022, **928**, 167202.

131 H. Jiang, Y. Xie, R. Zhu, Y. Luo, X. Sheng, D. Xie and Y. Mei, *Chem. Eng. J.*, 2023, **456**, 141049.

132 H. Yan, X. Fan, M. Cai, S. Song and M. Zhu, *J. Colloid Interface Sci.*, 2021, **602**, 131–145.

133 Y. Ning, D. Jian, S. Liu, F. Chen, Y. Song, S. Li and B. Liu, *Carbon*, 2023, **202**, 20–30.

134 Y. Wu, W. Zhao, S. Liu and L. Wang, *Chem. Eng. J.*, 2022, **438**, 135483.

135 H. Zhao, J. Ding, M. Zhou and H. Yu, *ACS Appl. Nano Mater.*, 2021, **4**, 3075–3086.

136 J. Wu, Y. Chen, L. Zhang and X. Sheng, *Prog. Org. Coat.*, 2023, **182**, 107706.

137 Y. Wu, L. Wu, W. Yao, B. Jiang, J. Wu, Y. Chen, X. Chen, Q. Zhan, G. Zhang and F. Pan, *Electrochim. Acta*, 2021, **374**, 137913.

138 M. Cai, X. Fan, H. Yan, Y. Li, S. Song, W. Li, H. Li, Z. Lu and M. Zhu, *Chem. Eng. J.*, 2021, **419**, 130050.

139 L. Shen, W. Zhao, K. Wang and J. Xu, *J. Hazard. Mater.*, 2021, **417**, 126048.

140 F. Zhang, W. Liu, S. Wang, H. Shi, C. Liu, L. Liang and K. Pi, *Polymer*, 2021, **230**, 124086.

141 X. He, S. Li, J. Wu, Y. Chen, L. Zhang and X. Sheng, *Ind. Eng. Chem. Res.*, 2022, **61**, 12576–12589.

142 X. He, J. Wu, S. Li, Y. Chen, L. Zhang and X. Sheng, *Prog. Org. Coat.*, 2022, **171**, 107042.

143 S. Li, H. Huang, F. Chen, X. He, Y. Ma, L. Zhang, X. Sheng, Y. Chen, E. Shchukina and D. Shchukin, *Prog. Org. Coat.*, 2021, **161**, 106478.

144 X. He, S. Li, R. Shen, Y. Ma, L. Zhang, X. Sheng, Y. Chen, D. Xie and J. Huang, *Adv. Compos. Hybrid Mater.*, 2022, **5**, 1699–1711.

145 J. Chen and W. Zhao, *Chem. Eng. J.*, 2021, **423**, 130195.

146 J. Wu, Y. Chen, L. Zhang and X. Sheng, *J. Ind. Eng. Chem.*, 2024, **129**, 424–434.

147 X. He, J. Wu, Y. Chen, L. Zhang and X. Sheng, *Appl. Surf. Sci.*, 2022, **603**, 154455.

148 D. S. Schulman, D. May-Rawding, F. Zhang, D. Buzzell, N. Alem and S. Das, *ACS Appl. Mater. Interfaces*, 2018, **10**, 4285–4294.

149 J. Ding, H. Zhao, X. Zhao, B. Xu and H. Yu, *J. Mater. Chem. A*, 2019, **7**, 13511–13521.

150 Z. Xia, G. Liu, Y. Dong and Y. Zhang, *Prog. Org. Coat.*, 2019, **133**, 154–160.

151 X. Zhao, B. Zhang, Z. Jin, C. Chen, Q. Zhu and B. Hou, *RSC Adv.*, 2016, **6**, 97512–97522.

152 F. Gao, A. Du, R. Ma, C. Lv, H. Yang, Y. Fan, X. Zhao, J. Wu and X. Cao, *Colloids Surf., A*, 2020, **587**, 124318.

153 Y. Jing, P. Wang, Q. Yang, Y. He and Y. Bai, *Mater. Res. Express*, 2019, **6**, 086473.

154 J. Ding, H. Zhao, X. Zhao, B. Xu and H. Yu, *J. Mater. Chem. A*, 2019, **7**, 13511–13521.

155 C. Chen, Y. He, G. Xiao, Y. Xia, H. Li and Z. He, *Appl. Surf. Sci.*, 2018, **444**, 511–521.

156 M. Motamed, S. Mohammadkhah, M. Ramezanzadeh, H. Eivaz Mohammadloo and B. Ramezanzadeh, *ACS Appl. Mater. Interfaces*, 2022, **14**, 31170–31193.

